ACS APPLIED MATERIALS & INTERFACES

Research Article

www.acsami.org

Selective Light-Induced Patterning of Carbon Nanotube/Silver Nanoparticle Composite To Produce Extremely Flexible Conductive Electrodes

Inhyuk Kim,[†,⊥] Kyoohee Woo,[*,‡,⊥] Zhaoyang Zhong,[†,‡] Eonseok Lee,[‡] Dongwoo Kang,[‡] Sunho Jeong,[§] Young-Man Choi,[∥] Yunseok Jang,[‡] Sin Kwon,[*,‡] and Jooho Moon[*,†]

[†]Department of Materials Science and Engineering, Yonsei University, Seoul 120-749, Republic of Korea

[‡]Advanced Manufacturing Systems Research Division, Korea Institute of Machinery and Materials, Daejeon 34103, Republic of Korea

[§]Division of Advanced Materials, Korea Research Institute of Chemical Technology, Daejeon 305-600, Republic of Korea

[∥]Department of Mechanical Engineering, Ajou University, Suwon-si, Gyeonggi-do 16490, Republic of Korea

S *Supporting Information*

ABSTRACT: Recently, highly flexible conductive features have been widely demanded for the development of various electronic applications, such as foldable displays, deformable lighting, disposable sensors, and flexible batteries. Herein, we report for the first time a selective photonic sintering-derived, highly reliable patterning approach for creating extremely flexible carbon nanotube (CNT)/silver nanoparticle (Ag NP) composite electrodes that can tolerate severe bending (20 000 cycles at a bending radius of 1 mm). The incorporation of CNTs into a Ag NP film can enhance not only the mechanical stability of electrodes but also the photonic-sintering efficiency when the composite is irradiated by intense pulsed light (IPL). Composite electrodes were patterned on various plastic substrates by a three-step process comprising coating, selective IPL irradiation, and wiping. A composite film selectively exposed to IPL could not be easily wiped from the substrate, because interfusion induced strong adhesion to the underlying polymer substrate. In contrast, a nonirradiated film adhered weakly to the substrate and was easily removed, enabling highly flexible patterned electrodes. The potential of our flexible electrode patterns was clearly demonstrated by fabricating a light-emitting diode circuit and a flexible transparent heater with unimpaired functionality under bending, rolling, and folding.

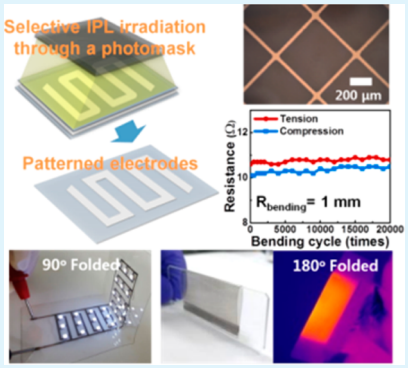

KEYWORDS: *carbon nanotube, Ag nanoparticle, composite, intense pulsed light irradiation, patterning, flexible conductive electrode*

INTRODUCTION

With increasing interest in highly flexible electronic devices such as foldable displays, flexible batteries, and wearable sensors, high-performance electrodes that are electrically stable under mechanical deformation are highly demanded.[1−8] Therefore, as alternatives to fragile and inflexible conductors, various flexible conducting materials, such as carbon nanotubes (CNTs),[9−12] graphene,[13−15] metal nanowires (NWs),[16−18] and nanocomposite materials,[19−23] have been studied. Among these, the composite—in which two or three flexible organic and highly conductive inorganic components are combined—is recognized as an effective strategy for developing high-performance electrodes or interconnects with high conductivity and mechanical stability. For example, in the case of a metal (e.g., Ag or Cu) nanoparticle (NP)/CNT composite system, the metal NPs mainly contribute to the conductivity, whereas the CNTs act as a conducting bridge between the metal NPs, resulting in preservation of the electrical property under mechanical stress.

In the fabrication of composite electrodes, patterning with clear definition over a large area is vital. Conventional lithographic techniques involving UV irradiation and chemical etching are widely used to produce microscale and nanoscale patterns; however, these methods have several disadvantages, including the use of expensive equipment, complex processes with multiple steps, and a low throughput.[24−26] In addition, the patterning of composite materials consisting of organic and inorganic components is difficult with such techniques because the etchant is generally designed to selectively react with one component (e.g., metal) of the composite. As an alternative to optical lithography, solution-based printing approaches such as inkjet printing, screen printing, transfer printing, gravure (offset) printing, and reverse-offset printing have been adopted for fabrication of composite electrode patterns.[27−31] However, despite their tremendous technical successes, issues remain unsolved, such as the imperfect control of defects and pattern shapes, low patterning resolution, and poor uniformity over large areas. In this regard, it is critical to develop more practical

Received: November 14, 2016
Accepted: February 1, 2017
Published: February 1, 2017

DOI: 10.1021/acsami.6b14580
ACS Appl. Mater. Interfaces 2017, 9, 6163−6170

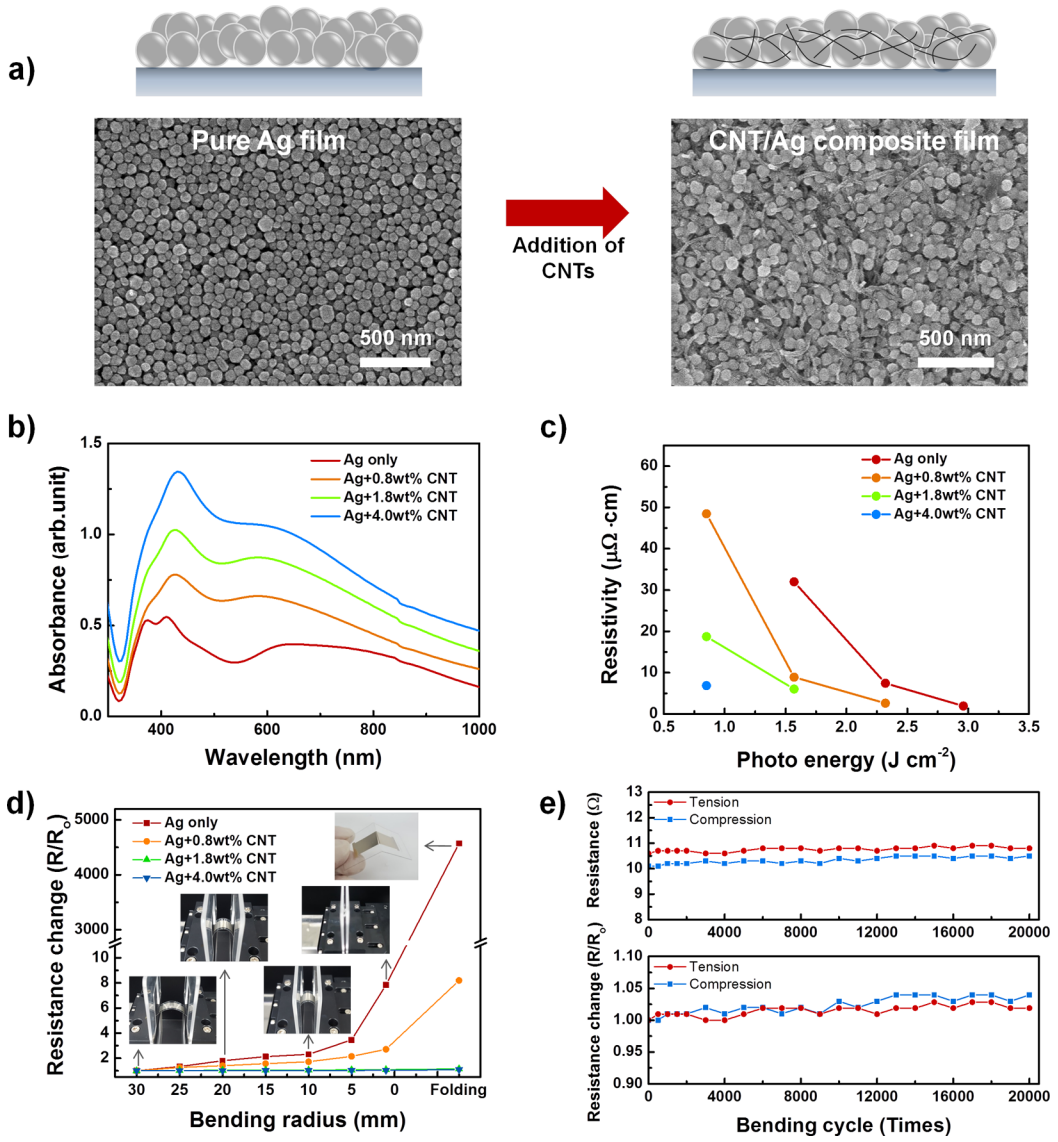

Figure 1. (a) Schematics and SEM surface images for (left) pure Ag NP film and (right) 1.8 wt % CNT-incorporated Ag NP composite film. (b) UV−vis spectra for CNT/Ag NP composite films with CNT concentrations of 0, 0.8, 1.8, and 4.0 wt %. (c) Resistivity variation of films with different CNT amounts as a function of IPL irradiation energy. (d) Electrical resistivity change (R/R_0) of films with CNT concentrations of 0, 0.8, 1.8, and 4.0 wt % under bending at various radii ranging from 0 (folding) to 30 mm. (Insets) Photographs of CNT/Ag NP composite films undergoing bending and folding tests. (e) Resistivity change of CNT (1.8 wt %)/Ag NP composite film as a function of bending cycles for up to 20 000 cycles with a fixed radius of 1 mm.

and simple pattering routes to obtain composite-based highly reliable flexible conductive features that are commercially viable for the next-generation electronics industry.

Photonic sintering, which involves intense pulsed light (IPL) with a broad spectrum in the visible range, has attracted great interest in the field of printed flexible electronics because it provides an effective route for the curing or sintering of large-area, solution-processed functional layers on heat-sensitive plastic substrates in a very short time of several milli-seconds.[32−36] Recently, in our previous study, after IPL irradiation, part of the thermal energy transformed from the high-photon energy of the IPL when it was absorbed by metal NWs was transferred to the underlying plastic substrate, which softened or even melted the surface of the substrate. Because of this thermal-energy transfer, NWs were self-nanoembedded into the polymer substrate, causing strong adhesion at the interface. Moreover, the patterning of NW-based flexible transparent electrodes has been readily accomplished on the basis of the significant difference in adhesion between IPL-irradiated and nonirradiated NW films.[37−39]

In this study, selective IPL photonic sintering was employed for the patterning of highly flexible conductive electrodes based on a multiwalled carbon nanotube (MWCNT)-reinforced Ag NP composite under severe mechanical conditions, such as bending, rolling, twisting, and folding deformations. By investigating the electrical and mechanical properties of the composite electrodes with respect to the CNT concentration, we confirmed that addition of CNTs over 1.8 wt % contributed to the maintenance of continuous electron pathways, which served as bridges connecting the cracked Ag conductive film resulting from mechanical deformation. In addition to this mechanical enhancement, the CNTs improved the photonic sintering efficiency of the CNT/Ag NP composite film during IPL irradiation, boosting the optical absorbance because of their

DOI: 10.1021/acsami.6b14580
ACS Appl. Mater. Interfaces 2017, 9, 6163−6170

low reflectance and high absorbance over a broad wavelength range.[40,41] After selective IPL exposure with a photomask, the IPL-irradiated CNT/Ag composite could not be easily wiped out, because of the strong adhesion caused by interfusion between the underlying polymer substrate and the composite film. In contrast, the nonirradiated region was readily removed from the substrate, enabling patterning of the composite electrode. Versatile patternability on a variety of plastic substrates with different glass transition temperatures (T_g) was demonstrated by controlling two key parameters (voltage and time) of the IPL process. The dominant parameter for developing patterns on various substrates was determined by understanding the relationship between the light energy required for patterning and the T_g of the substrate. The fabricated composite electrode patterns exhibited high electrical performance (6.1 $\mu\Omega$·cm) and excellent mechanical stability, enduring 20 000 bending cycles at a bending radius of 1 mm. Finally, the potential feasibility of the patterned flexible electrodes for various practical device applications was demonstrated. Our results not only provide an effective method for fabricating highly flexible electrode patterns over a large area but also facilitate their widespread application in future electronics, such as foldable displays, flexible batteries, and wearable sensors.

RESULTS AND DISCUSSION

CNT/Ag NP composite inks with various CNT concentrations (from 0.8 to 4.0 wt %) were prepared by mixing commercial Ag NP ink (ROS 420, N&B) and a MWCNT dispersion (Carbobyk, BYK). Composite films were successfully fabricated by spin-coating at 5000 rpm with the prepared inks. A pure Ag film was prepared for comparison with the composite films. Surface microstructures of pure Ag and CNT (1.8 wt %)/Ag NP composite films before thermal treatment were examined by field-emission scanning electron microscopy (FESEM). As shown in Figure 1a, the Ag nanoparticulate films had an average particle size of ~50 nm with high uniformity. In the composite film, the CNTs incorporated into the Ag NPs matrix were uniformly dispersed between Ag NPs, without severe aggregation.

Figure 1b shows UV−vis spectra of pure Ag NP film and CNT/Ag NP composite films with different CNT concentrations: 0.8, 1.8, and 4.0 wt %. For the pure Ag NP film, large absorption (absorption peak centered at 420 nm) in the wavelength range 330−550 nm was observed, which originated from the net effect of surface plasmon resonance of Ag NPs. With increasing CNT content, absorption intensity in the range 400−1000 nm gradually increased, as expected. This increased light absorption due to the added CNTs may have improved the IPL photonic sintering efficiency. To investigate this effect, Ag films with different CNT contents (0, 0.8, 1.8, and 4.0 wt %) were irradiated by single-pulsed IPL with various photonic energies. The photonic energy was controlled by adjusting the operating voltage (300, 340, 380, and 420 V) with a fixed exposure time of 1000 μs. The resistivity variation and microstructure evolution of the films with different CNT amounts were analyzed as a function of the IPL irradiation energy, as shown in Figure 1c and in Figure S1 and Table S1. When the pure Ag film was irradiated with IPL of 0.85 J·cm^{-2}, it exhibited an insulating characteristic, indicating that well-interconnected conductive pathways were not formed in the film because of insufficient irradiation energy for the sintering of Ag NPs. As the IPL photon energy increased to 1.57, 2.32, and 2.96 J·cm^{-2}, the resistivity of the films decreased to 31.89, 7.37, and 1.98 $\mu\Omega$·cm, respectively. However, unlike the pure Ag film, CNT/Ag NP composite films were peeled from the substrate or severely burned and blackened after irradiation of 2.96 J·cm^{-2} (Figure S1b). Moreover, as the CNT content increased to 0.8, 1.8, and 4.0 wt %, the photon energy needed to achieve high conductivity without damage decreased to 2.32, 1.57, and 0.85 J·cm^{-2}, respectively. With increasing CNT concentration, although the resistivity increased slightly from 2.69 to 6.86 $\mu\Omega$·cm because of the increasing contact resistance between the CNTs and Ag NPs, the photonic energy required for sintering the composite film decreased. This indicates that the IPL photonic-sintering efficiency was enhanced by the unique optical properties of CNTs, that is, their large light absorption and low reflectance in the entire region from far-UV (200 nm) to far-IR (200 μm).[10,40−42]

To confirm the enhancement of mechanical properties of the composite electrode through the incorporation of CNTs, films with various CNT concentrations ranging from 0 to 4.0 wt % were prepared. The prepared films were treated by IPL irradiation and then their flexibility was evaluated. The electrical resistivity change (R/R_0) under bending and folding conditions is shown in Figure 1d, where R_0 and R/R_0 are the initial resistance and resistance change, respectively. It should be noted that R_0 values for the composite films with different CNT amounts were measured as 3.1 Ω (0 wt %), 4.3 Ω (0.8 wt %), 10.2 Ω (1.8 wt %), and 12.7 Ω (4.0 wt %). For the pristine Ag NP film, the resistivity significantly increased as the bending radius decreased, exhibiting an approximately 8-fold increase at a bending radius of 1 mm and 4570 times increase under folding conditions. As CNTs were added, the variations in R/R_0 became diminished when various mechanical deformations were applied. For films with CNTs added at 0−0.8 wt %, the composite electrodes did not exhibit a remarkable flexibility enhancement (R/R_0 = 8 for film with 0.8 wt % CNTs under folding). At CNT concentrations greater than 1.8 wt %, the resistance value remained almost constant even when the film was bent at a 1 mm radius or folded. After 20 000 cyclic inner and outer bending tests at a bending radius of 1 mm with a frequency of 1.5 Hz, the 1.8 wt % CNT-incorporated Ag film exhibited little resistance change (R/R_0 = 1.04), as shown in Figure 1e. CNTs were located between intergranular cracks that were generated in the composite electrode before and after the 20 000 bending cycles, contributing to preservation of the effective electrical pathway between Ag grains (Figure S2). These results indicate that the added CNTs, with high mechanical strength and high aspect ratio, acted as conductive bridges for the Ag NP film, which was vulnerable to mechanical stress-induced cracking.

When the CNT/Ag NP composite film was irradiated by IPL, the photons of the instant IPL irradiation were absorbed by the composite film and then converted into thermal energy. Some of the heat energy was utilized to sinter the Ag NPs, and the remaining energy was transferred to the underlying polymer substrate. Thus, the surface of the substrate overlying the composite film exposed to IPL was softened or melted, allowing interfusion to occur at the interface between the composite film and the substrate, as shown in Figure 2a. Because of this interfusion, extremely strong adhesion between the IPL-irradiated composite film and the substrate was achieved. Furthermore, a conductive composite film was easily patterned by using this adhesion enhancement, as illustrated in Figure 2b. The as-coated CNT/Ag NP composite film was

DOI: 10.1021/acsami.6b14580
ACS Appl. Mater. Interfaces 2017, 9, 6163−6170

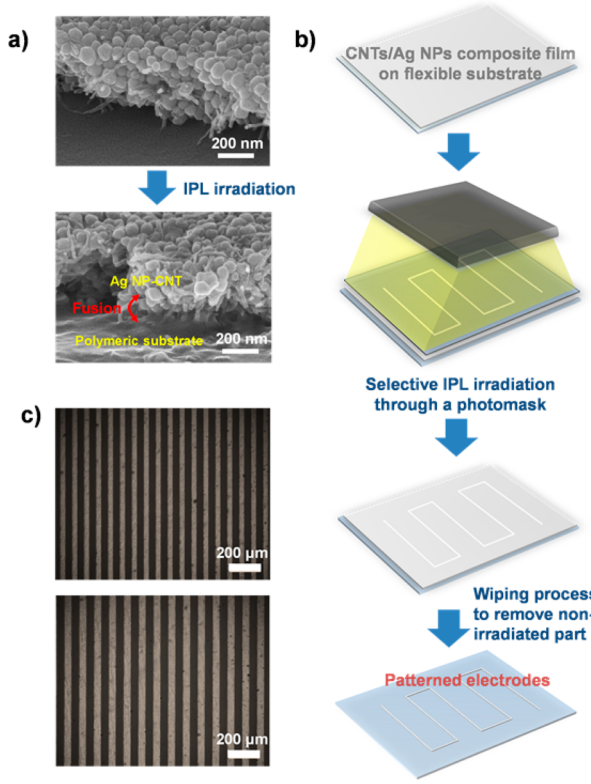

Figure 2. (a) Cross-sectional FESEM images of CNT (1.8 wt %)/Ag NP composite films before and after IPL irradiation. Interfusion between the composite and the polymer substrate occurred, resulting in strong adhesion at the interface. (b) Schematic showing the SLIP process. (c) Optical microscopic images for patterns with line widths of 30 and 50 μm fabricated by the SLIP process.

selectively exposed to IPL with a mask, followed by removal of the nonirradiated part of the film, which had poor adhesion with the underlying substrate, enabling the composite electrode to be patterned. We denoted this process as selective light-induced patterning (SLIP). To confirm the patternability of the SLIP process, the prepared CNT (1.8 wt %)/Ag NP composite film on poly(ethylene terephthalate) (PET) was shielded by a photomask having line patterns with widths of 30 and 50 μm and then irradiated by IPL (1.57 J·cm^{-2}) at 340 V for 1000 μs. After IPL irradiation, the nonirradiated area of the CNT/Ag NP film was selectively wiped off with a fabric dampened with ethanol, which was the main solvent of the CNT/Ag ink. Optical microscopy was performed to evaluate the developed patterns, as shown in Figure 2c. The line width of the patterns was measured to be ~31 and 52 μm. The width of the fabricated line was almost equal to the mask size, clearly indicating that the SLIP process enabled the reliable production of mechanically stable microscale electrode patterns over a large area. To determine the miniumum resolution of our SLIP process, a photomask with a pattern of 10 μm line width was prepared, and then it was observed that developed pattern had 16 μm line width (Figure S3). Slight widening of the pattern might be due to several factors such as light diffraction and thermal conduction, as explained in our previous report.[37]

The proposed SLIP process has several advantages over existing methods for the fabrication of conductive patterns. First, this process allows the fast, continuous, and large-area production of flexible conductive patterns because it is based on ultrafast photonic sintering using a large area-capable light source, which is unlikely to direct the laser writing process, in which a spatially limited laser beam should be repeatedly scanned. Second, it is a simple and eco-friendly process with little waste because it consists of just three stages (coating, selective IPL irradiation, and wiping) and does not involve complex steps or solutions such as photoresists, etchants, and developers, which are required in conventional photolithography. Additionally, whereas in conventional methods the conductive patterns are predefined by the printing processes, followed by additional heat-treatment for sintering of the NPs, post-treatment is unnecessary in our SLIP process because the NPs can be sintered during the patterning process. Third, the ink formulation is readily achievable without complex rheological requirements that should be met in traditional printing technologies, such as screen printing, inkjet printing, and reverse-offset printing. For example, the ink used in reverse-offset printing should be coatable on a hydrophobic blanket. Moreover, the surface energy of the coated film must be well-controlled for the offset steps, in which the unnecessary part of the coated film is removed by a patterned cliché with a high surface energy and then the pattern left on the blanket is transferred to a desired substrate. Various additives should be added to the ink for reverse-offset printing in consideration of its patterning mechanism.

However, because the ink used in the SLIP process only requires uniform coating ability, there are fewer constraints in the ink formulation. Supplementary agents, such as an adhesion promoter to enhance adhesion between the printed layer and the substrate, are unnecessary because strong adhesion can be spontaneously developed after IPL irradiation. Furthermore, the straightforward ink formulation offers relatively easy access to ink recycling. To verify that the ink is recyclable, the nonirradiated composite was collected after the wiping process. The wet fabric used for wiping material was immersed/washed in a bath filled with solvent (i.e., ethanol) to disperse the unsintered composite particles. The composite particles could be collected by centrifugation and then they were redispersed into the solvent. Finally, the recycled ink could be obtained after adjustment of its concentration. This ink was resubjected to the SLIP process, and the resulting coated and patterned electrodes appeared similar to those obtained with fresh ink, revealing that ink recycling was achieved (Figure 3). This indicates that the economic burden can be relieved even if an expensive noble metal (e.g., Ag)-based ink is used.

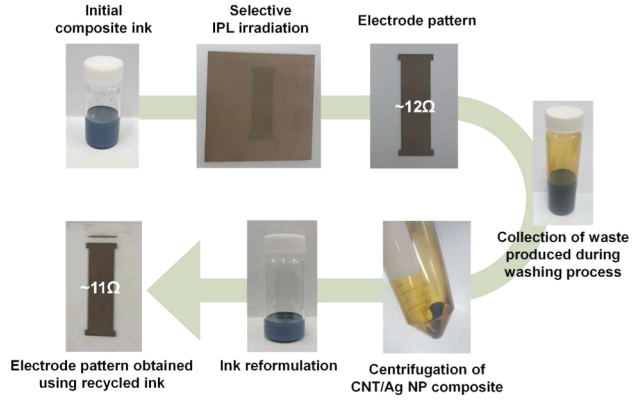

Figure 3. Procedure for verifying ink recyclability. Recycled ink exhibited a similar performance to freshly formulated ink.

DOI: 10.1021/acsami.6b14580
ACS Appl. Mater. Interfaces 2017, 9, 6163−6170

Finally, the proposed approach is favorable for obtaining well-defined conductive patterns with a sharp edge, flat surface, and accurate position with respect to the targeted position on the plastic substrate. The developed patterned surface was intactly flat, similar to the pristine surface of the as-spin-coated film, and its edge was sharp after the wiping process, as shown in Figure S4. Thermal shrinkage of the heat-sensitive plastic substrates that generally occurs during the post-treatment process for NP sintering was minimized because the heat was instantly generated on a selected IPL-irradiated area, allowing patterns to be developed on the plastic substrates with high positional accuracy. The positional error for conductive patterns (6 × 8 arrays) prepared by our SLIP process on a 100 × 100 cm^2 PET substrate was investigated, as shown in Figure S5. For comparison, the positional errors of the same patterns prepared by gravure printing and annealing at 100 °C for 15 min on a hot plate to develop conductivity were also considered. The length and direction of each arrow represent the positional error vectors of the resulting patterns with respect to the corresponding position of either the photomask pattern or the cliché. For the gravure-printed sample, a large positional error of 13.4 μm (in x-direction)/8.6 μm (in y-direction) was observed, which appears to be related to thermal shrinkage of the PET substrate, as all the error vectors point toward the center of the film. As the film size and annealing temperature increase, this positional error is expected to increase. However, for the sample fabricated by the SLIP process, the positional error was 5.9 μm (in x-direction)/5.6 μm (in y-direction), indicating that the substrate shrinkage had little influence.

Our SLIP process is based on interfusion at the interface between the composite film and the softened or melted polymer substrate. This means that the patternability is related to the glass transition temperature (T_g) of the polymeric substrate. The photo energy required for patterning on a high-T_g substrate is larger than that for a low-T_g substrate. To understand the relationship between the photo energy required for patterning and the T_g of the substrate, the patternability of a CNT (1.8 wt %)/Ag NP composite film on various plastic substrates with different T_g values—including PET (T_g = 120 °C), polycarbonate (PC, T_g = 155 °C), poly(ether sulfone) (PES, T_g = 230 °C), and polyimide (PI, T_g = 410 °C)—was investigated, as shown in Figure S6. The photo energy was controlled by adjusting the IPL processing parameters (operation voltage and duration) for a single pulsed flash of light. First, the total photo energy was modulated to 0.85, 1.57, 2.32, and 2.96 J·cm^{-2} by controlling the voltage (300, 340, 380, and 420 V, respectively) for a fixed duration of 1000 μs. When selective IPL irradiation (0.85 J·cm^{-2}) with 300 V was applied, the pattern was not well-developed on all types of substrates, because the patterns defined by the IPL-irradiated area were partially (on PET and PC) or completely (on PES and PI) washed away after the wiping process. This indicated that 0.85 J·cm^{-2} irradiation was insufficient to generate fusion between the composite film and the substrate. When the applied voltage was increased to 340 V (1.57 J·cm^{-2}), the pattern was developed on PET, PC, and PES substrates. However, the pattern was partially removed from the higher-T_g PI substrate by wiping. For additional photo energy to develop the pattern on PI, the voltage was increased to 380 V (2.32 J·cm^{-2}) and 420 V (2.96 J·cm^{-2}). However, in both voltage conditions, the composite layer was peeled (or burned) from all the substrates—including the PI substrate—during IPL irradiation, possibly because the photo energy was too high. These observations indicate that there is a minimum threshold voltage, below which insufficient fusion is generated, and a maximum threshold voltage, above which peeling or burning of the composite film occurs during IPL irradiation. Consequently, controlling the voltage to provide a desirable energy for developing patterns on high-T_g substrates may be an ineffective method with a relatively narrow processing window.

Instead of controlling the voltage, the exposure time was varied in the range 300−2000 μs. The power-supply voltage was fixed to 340 V, which was considered to be between the minimum and maximum threshold values. As shown in Figure S6b, when the irradiation duration ranged from 500 (0.71 J·cm^{-2}) to 2000 μs (2.96 J·cm^{-2}), the pattern was well-developed on the PET substrate, although its line width increased slightly. The pattern was developed on PC, PES, and PI substrates for durations of 600−2000, 800−2000, and 1900−2000 μs, respectively. Interestingly, although the total light energy (0.71 J·cm^{-2}) for the condition of 340 V/500 μs was lower than that (0.85 J·cm^{-2}) for 300 V/1,000 μs, patterning was possible on the PET substrate. In addition, the total energy (2.96 J·cm^{-2}) of light operated at 340 V/2000 μs was the same as that for 420 V/1000 μs, but the pattern was well-formed without peeling or burning during the IPL irradiation. This implies that although the total energy was the same, the operating voltage should be between the minimum and maximum thresholds for patterning, and control of the duration enables more convenient patterning on substrates with various T_g values owing to the relatively broad processing window. The patternability of the composite film on various substrates depended on the irradiation photo energy, which was controlled by the duration, as summarized in Figure 4a. At a photo energy in the range 0.51−2.96 J·cm^{-2}, all the substrates exhibited conductivity. However, the energy required for patterning changed according to the T_g of the substrate. In the case of PET (T_g = 120 °C), patterning was possible at a relatively low photo energy (0.71 J·cm^{-2}). As T_g increased to 150 °C (PC), 230 °C (PES), and 410 °C (PI), the photo energy required for patterning increased to 0.85, 1.23, and 2.74 J·cm^{-2}, respectively. This reveals that substrates with a higher T_g require a higher photo energy for patterning. The photo energy is plotted with respect to T_g in Figure 4b. By use of a linear regression, the relationship between the photo energy (joules per square centimeter) and T_g was obtained:

$$\text{photo energy} = 0.0076x - 0.24 \quad (1)$$

where x is the T_g of the substrate. By use of this equation, the photo energy required for patterning can be estimated.

The CNT (1.8 wt %)/Ag NP composite-based highly flexible conductive pattern derived from the SLIP process was successfully employed to construct a flexible light-emitting diode (LED) circuit and a flexible transparent heater (FTH), as shown in Figure 5. The LED circuit was fabricated by integrating 24 LED chips with flexible conductive patterns on a PC substrate with an area of 35 mm × 120 mm, and then its flexibility was evaluated, as shown in Figure 5a. The LED illumination intensity remained without significant degradation even when the electrode pattern of the circuit was bent, twisted, rolled, and folded. As another application, a FTH was fabricated by use of a mesh-patterned electrode with a line width of ∼45 μm over an area of 50 mm × 50 mm, as shown in Figure 5b. The prepared mesh-patterned film exhibited a transmittance of ∼80% and a sheet resistance (R_S) of ∼3 Ω/sq (Figure S7). A

DOI: 10.1021/acsami.6b14580
ACS Appl. Mater. Interfaces 2017, 9, 6163−6170

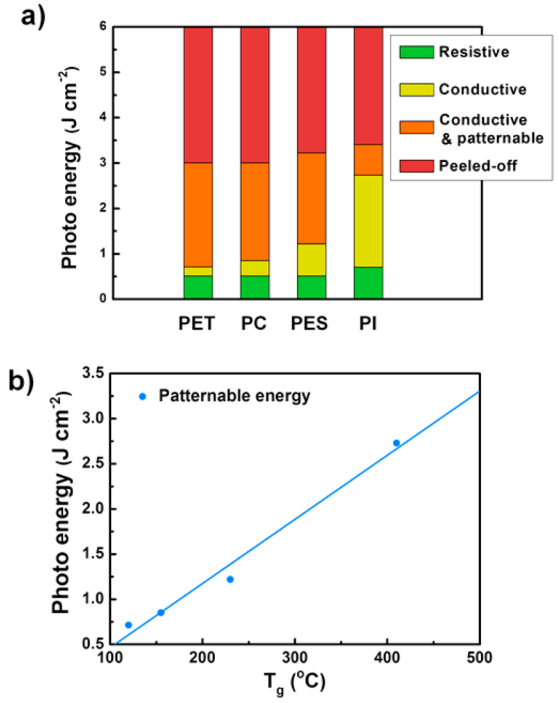

Figure 4. (a) Patternability of CNT (1.8 wt %)/Ag NP composite films fabricated on various substrates with varying irradiation photo energies. (b) Plot of photo energy required for patterning with respect to the T_g of the substrate (blue dots). A linear regression was performed to derive the equation for the required photo energy as a function of T_g (blue line).

direct-current bias voltage of 3 V was applied at both ends of the mesh-patterned film to induce electrically driven resistive Joule heating. The FTH with mesh patterns exhibited uniform heating over the entire region, indicating a uniform R_S distribution on the film. The heating operation of the FTH under bending and folding at angles of 90° and 180° was highly stable, with little change in electrical property. This indicates that our easily patterned CNT/Ag NP composite electrode has electrical conductivity and mechanical compliance, as well as potential for practical use in real flexible electronics.

CONCLUSIONS

In summary, we demonstrated the fabrication of CNT/Ag NP-based highly flexible conductive patterns using a simple SLIP process comprising only three steps (coating, selective IPL irradiation, and wiping). The incorporation of CNTs into the Ag NP film not only enhanced the mechanical stability of the electrodes but also improved the photonic sintering efficiency when the composite was irradiated by IPL. The resistance of the fabricated composite electrode was almost constant under 20 000 bending cycles at a bending radius of 1 mm. Several advantages of the proposed SLIP process were meticulously identified, including ecocompatibility, ease of ink recycling, precise patternability with high positional accuracy, and compatibility with roll-to-roll, fast, and large-area processes. In addition, the SLIP method can be applied to various plastic substrates (PET, PC, PES, and PI) by controlling the light energy. Composite electrode patterns obtained via SLIP exhibited high conductivity and durable mechanical stability under various deformation conditions (bending, twisting, and folding). A flexible LED array circuit and an FTH were successfully demonstrated for CNT/Ag conductive electrodes patterned by the SLIP process. Our readily achievable ink and facile patterning approach for fabricating highly robust,

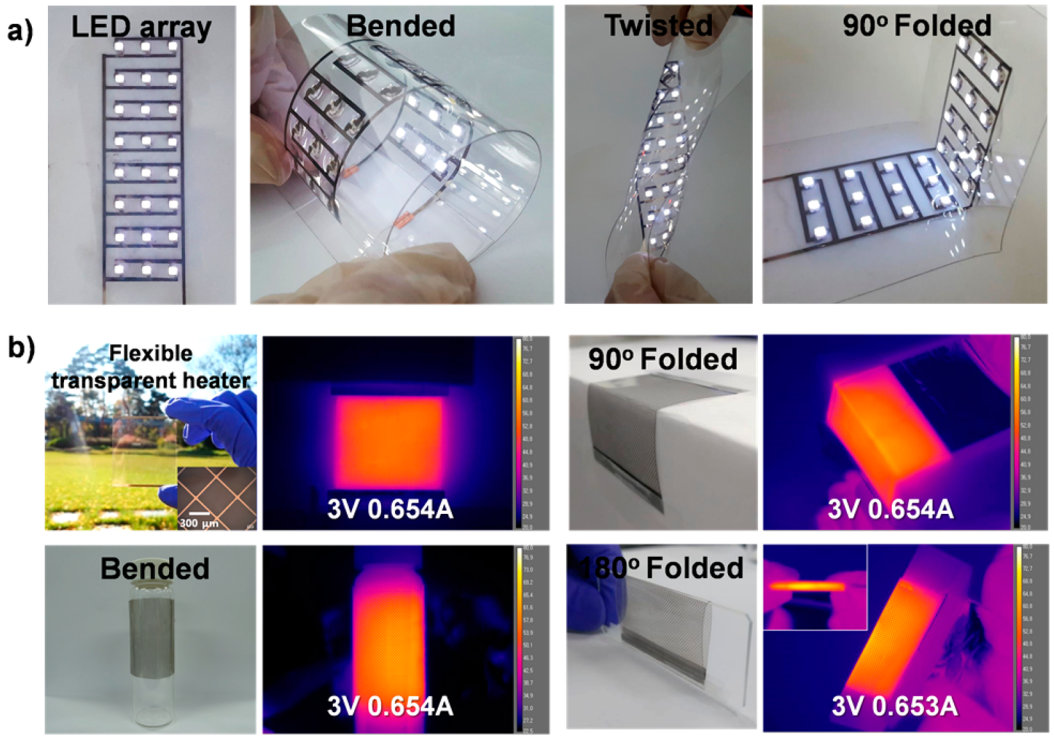

Figure 5. Photographs of (a) LED array circuit and (b) FTH with CNT (1.8 wt %)/Ag NP composite-based conductive patterns. The devices operated stably under various deformation conditions.

DOI: 10.1021/acsami.6b14580
ACS Appl. Mater. Interfaces 2017, 9, 6163−6170

extremely flexible conductive patterns can greatly invigorate the flexible-electronics industry.

METHODS

Fabrication of Conductive CNT/Ag NP Patterns. CNT/Ag NP composite inks were fabricated from a commercial ethanol-based Ag-NP ink (50 nm, ROS 420, N&B) and an aqueous CNT-dispersion ink (Carbobyk, BYK). The CNT-dispersion ink was composed of 8 wt % MWCNT dispersed in water. CNT-dispersion inks exhibit the dispersion property in ethanol. We added 0−4.0 wt % CNTs into the ethanol-based Ag-NP dispersion inks, followed by ultrasonication for uniform dispersion. After 30 min, the obtained Ag NP-CNT composite inks were deposited by spin-coating on polyester (Tetoron KEL86W, Teijin DuPont Films), PC (C100, Sejin T.S. Co., Ltd.), PES (Glastic SCL120, I-Components Co., Ltd.), and PI (KYPI, Suzhou Kying Industrial Materials Co., Ltd.) substrates. The resulting thin films were dried at 50 °C for 15 min under ambient conditions by use of a hot plate. A fabricated Ag/CNT composite film was annealed and patterned by use of a photonic sintering system (PulseForge 1300, Novacentrix) with a xenon flash lamp of broadband wavelength 200−1500 nm. A quartz photomask (comprising a patterned chrome masking layer) was then placed on the thin film, and the film was exposed to IPL irradiation at 0.51−3.41 $J \cdot cm^{-2}$ (with varying CNT concentrations from 0 to 4.0 wt %). To remove the nonirradiated region, the annealed films were wiped by a fabric soaked with ethanol.

Characterization of CNT/Ag Composite Pattern. The surface and cross-sectional morphology of the synthesized film were observed by high-resolution FESEM (S4800, Hitachi Ltd.) and on a confocal microscope (Optelicsr C130, Lasertec). The sheet resistance and film thickness were measured with a noncontact eddy-current probe system (EC-80-P model, Napson Corp.) and a surface-profiling system ($P\bar{6}$, KLA Tencor). The resistivity value of electrodes was determined by using the average sheet resistance measured 10 times per sample. Absorbance of the films was measured on a UV−vis spectrophotometer (Lambda 750S model, PerkinElmer Inc.) with a wavelength range of 300−1000 nm. The flexibility of the composite pattern was confirmed by cyclic bending tests with a custom-built automatic bending tester (iPen Co., Ltd.).

Fabrication of LED Array. First, the flexible composite pattern for the LED array was fabricated on the PC film via the SLIP process. Then, 24 white LED chips (PCL-C4W CZ31SA, Power LighTec) were attached to the flexible circuit with silver paste (ELCOAT A-201, Cans). The LEDs were operated by a power-supply unit (HM 7044, HAMEG Instruments).

Fabrication of FTH. A CNT/Ag NP composite mesh pattern was developed on a PET substrate by use of the prepared mesh-patterned photomask. Both sides of the pattern were connected to a power-supply unit (HM 7044, HAMEG Instruments) with copper conductive tape. The fabricated thermal heater had a series resistance of ∼4.6 Ω. The transmittance of the mesh heater was measured to be 80% on a UV−vis spectrophotometer (Lambda 750S model, PerkinElmer Inc.) with a wavelength range of 200−1000 nm. Thermal heating performance was observed in real time by use of an IR camera (A600 series, FLIR Systems, Inc.).

ASSOCIATED CONTENT

Supporting Information

The Supporting Information is available free of charge on the ACS Publications website at DOI: 10.1021/acsami.6b14580.

One table listing process conditions, electrical properties, and thicknesses of composite films; seven figures showing surface FESEM images and photographs of films after IPL sintering and bending tests, images of patterned composite line with photo masks, optical microscopic image and height profile of patterns, surface profile and position-error vector data for SLIP-prepared patterned electrode, photographs showing the resulting serpentine line patterns on various plastic substrates, and transmittance vs wavelength plot for IPL-treated mesh pattern (PDF)

AUTHOR INFORMATION

Corresponding Authors

*E-mail khwoo@kimm.re.kr; tel +82-42-868-7615; fax +82-42-868-7176 (K.W.).

*E-mail skwon@kimm.re.kr; tel +82-42-868-7219; fax +82-42-868-7176 (S.K.).

* E-mail jmoon@yonsei.ac.kr; tel +82-2-2123-2855; fax +82-2-312-5375 (J.M.).

ORCID

Jooho Moon: 0000-0002-6685-9999

Author Contributions

⊥I.K. and K.W. contributed equally.

Notes

The authors declare no competing financial interest.

ACKNOWLEDGMENTS

This work was supported by the Ministry of Trade, Industry & Energy (MOTIE, Korea) under Advanced Technology Center (ATC) Program (10067668) and Technology Innovation Program (10052802). It was also supported by a National Research Foundation of Korea (NRF) funded by the Korean government (MSIP) (2012R1A3A2026417).

REFERENCES

(1) Liang, J.; Li, L.; Niu, X.; Yu, Z.; Pei, Q. Elastomeric Polymer Light-Emitting Devices and Displays. *Nat. Photonics* **2013**, *7*, 817−824.

(2) Choi, D. Y.; Kang, H. W.; Sung, H. J.; Kim, S. S. Annealing-free, Flexible Silver Nanowire−Polymer Composite Electrodes via a Continuous Two-step Spray-coating Method. *Nanoscale* **2013**, *5*, 977−983.

(3) Chen, Z.; To, J. W. F.; Wang, C.; Lu, Z.; Liu, N.; Chortos, A.; Pan, L.; Wei, F.; Cui, Y.; Bao, Z. A Three-Dimensionally Interconnected Carbon Nanotube-Conducting Polymer Hydrogel Network for High-Performance Flexible Battery Electrodes. *Adv. Energy Mater.* **2014**, *4*, No. 1400207.

(4) Kim, J.-S.; Ko, D.; Yoo, D.-J.; Jung, D. S.; Yavuz, C. T.; Kim, N.-I.; Choi, I.-S.; Song, J. Y.; Choi, J. W. A Half Millimeter Thick Coplanar Flexible Battery with Wireless Recharging Capability. *Nano Lett.* **2015**, *15*, 2350−2357.

(5) Wang, Z.; Wu, Z.; Bramnik, N.; Mitra, S. Fabrication of High-Performance Flexible Alkaline Batteries by Implementing Multiwalled Carbon Nanotubes and Copolymer Separator. *Adv. Mater.* **2014**, *26*, 970−976.

(6) Wang, Y.; Wang, L.; Yang, T.; Li, X.; Zang, X.; Zhu, M.; Wang, K.; Wu, D.; Zhu, H. Wearable and Highly Sensitive Graphene Strain Sensors for Human Motion Monitoring. *Adv. Funct. Mater.* **2014**, *24*, 4666−4670.

(7) Yao, S.; Zhu, Y. Wearable Multifunctional Sensors using Printed Stretchable Conductors Made of Silver Nanowires. *Nanoscale* **2014**, *6*, 2345−2352.

(8) Savagatrup, S.; Chan, E.; Renteria-Garcia, S. M.; Printz, A. D.; Zaretski, A. V.; O'Connor, T. F.; Rodriquez, D.; Valle, E.; Lipomi, D. J. Plasticization of PEDOT:PSS by Common Additives for Mechanically Robust Organic Solar Cells and Wearable Sensors. *Adv. Funct. Mater.* **2015**, *25*, 427−436.

(9) Park, S.; Vosguerichian, M.; Bao, Z. A Review of Fabrication and Applications of Carbon Nanotube Film-Based Flexible Electronics. *Nanoscale* **2013**, *5*, 1727−1752.

(10) Cho, D.-Y.; Eun, K.; Choa, S.-H.; Kim, H.-K. Highly Flexible and Stretchable Carbon Nanotube Network Electrodes Prepared by

DOI: 10.1021/acsami.6b14580
ACS Appl. Mater. Interfaces 2017, 9, 6163−6170

Simple Brush Painting for Cost-effective Flexible Organic Solar Cells. *Carbon* **2014**, *66*, 530−538.
(11) Sun, D. M.; Liu, C.; Ren, W.-C.; Cheng, H.-M. A Review of Carbon Nanotube- and Graphene-Based Flexible Thin-Film Transistors. *Small* **2013**, *9*, 1188−1205.
(12) Lau, P. H.; Takei, K.; Wang, C.; Ju, Y.; Kim, J.; Yu, Z.; Takahashi, T.; Cho, G.; Javey, A. Fully Printed, High Performance Carbon Nanotube Thin-Film Transistors on Flexible Substrates. *Nano Lett.* **2013**, *13*, 3864−3869.
(13) Liu, F.; Song, S.; Xue, D.; Zhang, H. Folded Structured Graphene Paper for High Performance Electrode Materials. *Adv. Mater.* **2012**, *24*, 1089−1094.
(14) El-Kady, M. F.; Strong, V.; Dubin, S.; Kaner, R. B. Laser Scribing of High-Performance and Flexible Graphene-Based Electrochemical Capacitors. *Science* **2012**, *335*, 1326−1330.
(15) Niu, Z.; Zhang, L.; Liu, L.; Zhu, B.; Dong, H.; Chen, X. All-Solid-State Flexible Ultrathin Micro-Supercapacitors Based on Graphene. *Adv. Mater.* **2013**, *25*, 4035−4042.
(16) Kim, T.; Kim, Y. W.; Lee, H. S.; Kim, H.; Yang, W. S.; Suh, K. S. Uniformly Interconnected Silver-Nanowire Networks for Transparent Film Heaters. *Adv. Funct. Mater.* **2013**, *23*, 1250−1255.
(17) Sachse, C.; Weiß, N.; Gaponik, N.; Müller-Meskamp, L.; Eychmüller, A.; Leo, K. ITO-Free, Small-Molecule Organic Solar Cells on SprayCoated Copper-Nanowire-Based Transparent Electrodes. *Adv. Energy Mater.* **2014**, *4*, No. 1300737.
(18) Won, Y.; Kim, A.; Lee, D.; Yang, W.; Woo, K.; Jeong, S.; Moon, J. Annealing-Free Fabrication of Highly Oxidation-resistive Copper Nanowire Composite Conductors for Photovoltaics. *NPG Asia Mater.* **2014**, *6*, No. e105.
(19) Kuilla, T.; Bhadra, S.; Yao, D.; Kim, N. H.; Bose, S.; Lee, J. H. Recent Advances in Graphene Based Polymer Composites. *Prog. Polym. Sci.* **2010**, *35*, 1350−1375.
(20) Mackiewicz, N.; Surendran, G.; Remita, H.; Keita, B.; Zhang, G.; Nadjo, L.; Hagège, A.; Doris, E.; Mioskowski, C. Supramolecular Self-Assembly of Amphiphiles on Carbon Nanotubes: A Versatile Strategy for the Construction of CNT/Metal Nanohybrids, Application to Electrocatalysis. *J. Am. Chem. Soc.* **2008**, *130*, 8110−8111.
(21) Xu, C.; Wang, X.; Zhu, J. Graphene−Metal Particle Nanocomposites. *J. Phys. Chem. C* **2008**, *112*, 19841−19845.
(22) Peng, C.; Zhang, S.; Jewell, D.; Chen, G. Z. Carbon Nanotube and Conducting Polymer Composites for Supercapacitors. *Prog. Nat. Sci.* **2008**, *18*, 777−788.
(23) Wang, J.; Dai, J.; Yarlagadda, T. Carbon Nanotube−Conducting-Polymer Composite Nanowires. *Langmuir* **2005**, *21*, 9−12.
(24) Ouyang, S.; Xie, Y.; Wang, D.; Zhu, D.; Xu, X.; Tan, T.; DeFranco, J.; Fong, H. H. Photolithographic Patterning of Highly Conductive PEDOT:PSS and its Application in Organic Light-Emitting Diodes. *J. Polym. Sci., Part B: Polym. Phys.* **2014**, *52*, 1221−1226.
(25) Yin, Z.; Cheng, E.; Zou, H. A Novel Hybrid Patterning Technique for Micro and Nanochannel Fabrication by Integrating Hot Embossing and Inverse UV Photolithography. *Lab Chip* **2014**, *14*, 1614−1621.
(26) Ouyang, S.; Xie, Y.; Zhu, D.; Xu, X.; Wang, D.; Tan, T.; Fong, H. H. Photolithographic Patterning of PEDOT:PSS with a Silver Interlayer and its Application in Organic Light Emitting Diodes. *Org. Electron.* **2014**, *15*, 1822−1827.
(27) Kuang, M.; Wang, J.; Bao, B.; Li, F.; Wang, L.; Jiang, L.; Song, Y. Inkjet Printing Patterned Photonic Crystal Domes for Wide Viewing-Angle Displays by Controlling the Sliding Three Phase Contact Line. *Adv. Opt. Mater.* **2014**, *2*, 34−38.
(28) Sameenoi, Y.; Nongkai, P. N.; Nouanthavong, S.; Henry, C. S.; Nacapricha, D. One-step Polymer Screen-Printing for Microfluidic Paper-Based Analytical Device (μPAD) Fabrication. *Analyst* **2014**, *139*, 6580−6588.
(29) Choi, M. K.; Park, I.; Kim, D. C.; Joh, E.; Park, O. K.; Kim, J.; Kim, M.; Choi, C.; Yang, J.; Cho, K. W.; Hwang, J.-H.; Nam, J.-M.; Hyeon, T.; Kim, J. H.; Kim, D.-H. Thermally Controlled, Patterned Graphene Transfer Printing for Transparent and Wearable Electronic/Optoelectronic System. *Adv. Funct. Mater.* **2015**, *25*, 7109−7118.
(30) Secor, E. B.; Lim, S.; Zhang, H.; Frisbie, C. D.; Francis, L. F.; Hersam, M. C. Gravure Printing of Graphene for LargeCCArea Flexible Electronics. *Adv. Mater.* **2014**, *26*, 4533−4538.
(31) Kang, D.; Lee, E.; Kim, H.; Choi, Y.-M.; Lee, S.; Kim, I.; Yoon, D.; Jo, J.; Kim, B.; Lee, T.-M. Investigation on Synchronization of the Offset Printing Process for Fine Patterning and Precision Overlay. *J. Appl. Phys.* **2014**, *115*, No. 234908.
(32) Kang, H.; Sowade, E.; Baumann, R. R. Direct Intense Pulsed Light Sintering of Inkjet-Printed Copper Oxide Layers within Six Milliseconds. *ACS Appl. Mater. Interfaces* **2014**, *6*, 1682−1687.
(33) Song, C.-H.; Ok, K.-H.; Lee, C.-J.; Kim, Y.; Kwak, M.-G.; Han, C. J.; Kim, N.; Ju, B.-K.; Kim, J.-W. Intense-Pulsed-Light Irradiation of Ag Nanowire-Based Transparent Electrodes for Use in Flexible Organic Light Emitting Diodes. *Org. Electron.* **2015**, *17*, 208−215.
(34) Jo, Y.; Oh, S.-J.; Lee, S. S.; Seo, Y.-H.; Ryu, B.-H.; Moon, J.; Choi, Y.; Jeong, S. Extremely Flexible, Printable Ag Conductive Features on PET and Paper Substrates via Continuous Millisecond Photonic Sintering in a Large Area. *J. Mater. Chem. C* **2014**, *2*, 9746−9753.
(35) Abbel, R.; Teunissen, P.; Rubingh, E.; van Lammeren, T.; Cauchois, R.; Everaars, M.; Valeton, J.; van de Gejin, S.; Groen, P. Industrial-Scale Inkjet Printed Electronics Manufacturing-Production Up-Scaling from Concept Tools to a Roll-to-Roll Pilot Line. *Transl. Mater. Res.* **2014**, *1*, No. 015002.
(36) Perelaer, J.; Abbel, R.; Wünscher, S.; Jani, R.; van Lammeren, T.; Schubert, U. S. Roll-to-Roll Compatible Sintering of Inkjet Printed Features by Photonic and Microwave Exposure: from Non-Conductive Ink to 40% Bulk Silver Conductivity in Less than 15 Seconds. *Adv. Mater.* **2012**, *24* (19), 2620−2625.
(37) Zhong, Z.; Lee, H.; Kang, D.; Kwon, S.; Choi, Y.-M.; Kim, I.; Kim, K.-Y.; Lee, Y.; Woo, K.; Moon, J. Continuous Patterning of Copper Nanowire-Based Transparent Conducting Electrodes for Use in Flexible Electronic Applications. *ACS Nano* **2016**, *10*, 7847−7854.
(38) Zhong, Z.; Woo, K.; Kim, I.; Hwang, H.; Kwon, S.; Choi, Y.-M.; Lee, Y.; Lee, T.-M.; Kim, K.; Moon, J. Roll-to-Roll-Compatible, Flexible, Transparent Electrodes Based on Self-Nanoembedded Cu Nanowires Using Intense Pulsed Light Irradiation. *Nanoscale* **2016**, *8*, 8995−9003.
(39) Song, C.-H.; Han, C. J.; Ju, B.-K.; Kim, J.-W. Photoenhanced Patterning of Metal Nanowire Networks for Fabrication of Ultra-flexible Transparent Devices. *ACS Appl. Mater. Interfaces* **2016**, *8*, 480−489.
(40) Gokhale, V. J.; Shenderova, O. A.; McGuire, G. E.; Rais-Zadeh, M. Infrared Absorption Properties of Carbon Nanotube/Nano-diamond Based Thin Film Coatings. *J. Microelectromech. Syst.* **2014**, *23*, 191−197.
(41) Xu, Y.; Huang, S.; Ji, H.; Jing, L.; He, M.; Xu, H.; Zhang, Q.; Li, H. Facile Synthesis of CNT/AgI with Enhanced Photocatalytic Degradation and Antibacterial Ability. *RSC Adv.* **2016**, *6*, 6905−6914.
(42) Wang, S.; Zhang, A.; Peng, L. Doping-Free Carbon Nanotube Optoelectronic Devices. *Chin. Sci. Bull.* **2012**, *57*, 149−156.

DOI: 10.1021/acsami.6b14580
ACS Appl. Mater. Interfaces 2017, 9, 6163−6170